Pergamon

Bioorganic & Medicinal Chemistry 10 (2002) 2693–2704

BIOORGANIC & MEDICINAL CHEMISTRY

Synthesis, Characterization and Antitumor Studies of Transition Metal Complexes of *o*-Hydroxydithiobenzoate

Anuraag Shrivastav,[a] Nand K. Singh[a,*] and Geeta Srivastava[b]

[a]*Department of Chemistry, Banaras Hindu University, Varanasi, 221005, India*
[b]*Alberta Research Council, Edmonton, Alberta, Canada T6N 1E4*

Received 17 December 2001; accepted 7 March 2002

Abstract—*o*-Hydroxydithiobenzoate (*o*-HOdtb) forms complexes, [Ni(*o*-HOdtb)(*o*-HOdtbS)], [Cu(*o*-Odtb)], [Co(*o*-HOdtb)$_3$], [Fe$_2$(*o*-Odtb)$_3$], [Bu$^n_4$N][V(*o*-Odtb)$_3$] and [Bu$^n_4$N][Zn(*o*-HOdtb)$_3$] which were characterized by analyses and physicochemical studies. The bonding sites of *o*-HOdtb and the geometry of the complexes were determined by magnetic susceptibility, IR, ESR, NMR, Mössbauer and electronic spectral data. The structure of [Bu$^n_4$N][Zn(*o*-HOdtb)$_3$] and H$_2$C(*o*-HOdtb)$_2$ were assigned by single crystal X-ray diffraction studies. The monomeric complex [Bu$^n_4$N][Zn(*o*-HOdtb)$_3$] crystallizes in Pna2$_1$ space group. The Mössbauer spectra of [Fe$_2$(*o*-Odtb)$_3$] at 298 and 80 K suggest the presence of high spin iron(III) with an $S = 5/2$ state. All the metal complexes were observed to inhibit the growth of tumor in vitro, whereas, ligand did not. In vivo administration of these complexes resulted in prolongation of survival of tumor-bearing mice. Tumor bearing mice administered with metal complexes showed reversal of tumor growth associated induction of apoptosis in lymphocytes. The paper discusses the possible mechanisms and therapeutic implication of the ligand and its metal complexes in tumor regression and tumor growth associated immunosuppression.

Introduction

A number of compounds affect the biological properties of nucleic acid at the molecular level through physicochemical interaction or covalent binding.[1] Some cytotoxic drugs are believed to exert their activity through covalent binding to DNA, impairing many vital cellular functions.[2] The ability of covalent DNA adducts to alter RNA transcription has profound consequences for other cellular functions. There is evidence indicating that both the transcriptional control of the cell cycle[3] and the RNA content in the eukaryotic cell are closely related to the cell cycle kinetics.[4] Transcriptional as well as replication assays were used to characterize the covalent interaction of cisplatin, *trans*-DDP and ammineruthenium complexes with DNA.[5]

A connection between metal chelation and at least some types of cancer was suggested by Furst in 1963,[6] and in 1966 Schubert observed that metal chelation apparently plays a definite role in the cause and treatment of malignancy.[7] Ni(II) and Pd(II) complexes of diethyldithiophosphate displayed carcinostatic activity in the Walker 256 carcinosarcoma test.[8] Livingstone et al. reported that the palladium(II) and copper(II) chelates of the derivatives of dithiocarbazic acid, were found to display cytostatic activity in the 9KB test—a human epidermoid carcinoma of the nasopharynx.[9] Pd(II), Cu(II) and Zn(II) chelates of derivatives of *S*-methyldithiocarbazates have significant antitumor activity against P388 lymphoid leukemia in mice.[10] The most common side effects of a cisplatin therapy include kidney and gastrointestinal problems, including nausea, which may be attributed to the inhibition of enzymes through coordination of the heavy metal platinum to sulfhydryl groups in proteins. Accordingly a treatment with these metal chelates may counteract these symptoms.[11–13] We have earlier reported the synthesis and characterization of binary and heterobimetallic complexes of dithiofuroate and *p*-hydroxydithiobenzoate with 3d-metal ions. These complexes were tested for their inhibitory effect on ^{3}H-thymidine and ^{3}H-uridine incorporation in P815, a murine tumor cell line, in vitro at 1 and 5 μg/mL doses. The complexes of iron(III), nickel(II), copper(II) and zinc(II) have shown equitoxicity to P815 cells at high dose (5 μg/mL) while at low dose (1 μg/mL) these are less toxic and show significant inhibition in terms of ^{3}H-thymidine incorporation. However, manganese(II) complexes showed a proliferation effect at low dose.[14] We report here the synthesis, characterization, structure

*Corresponding author. E-mail: anuraagshrivastav@yahoo.com

0968-0896/02/$ - see front matter
PII: S0968-0896(02)00087-1

Table 1. Analytical data and physical properties of complexes of *o*-hydroxydithiobenzoate

Compound	Color	Mp (°C)	Yield (%)	Found (calcd) (%)					μ_{eff} (BM)	*m/z*
				M	S	C	H	N		
$[Bu^n_4N(o\text{-HOdtb})]$	Brown	98	90	—	15.9 (15.6)	67.3 (67.2)	10.1 (10.0)	3.2 (3.4)	—	—
$H_2C(o\text{-HOdtb})_2]$	Yellow	90	58	—	36.3 (36.4)	51.1 (51.1)	3.5 (3.4)	—	—	—
$[Bu^n_4N][V(o\text{-Odtb})_3]$	Maroon	83–85	78	7.1 (6.4)	24.7 (24.0)	55.2 (55.7)	5.8 (6.0)	1.8 (1.9)	Dia	797
$[Fe_2(o\text{-Odtb})_3]$	Black	110–113	76	18.9 (18.1)	32.0 (31.2)	40.7 (40.9)	1.8 (1.9)	—	5.9	613
$[Co(o\text{-HOdtb})_3]$	Black	137–139	91	11.1 (10.4)	33.3 (33.9)	44.6 (44.5)	2.4 (2.6)	—	Dia	—
$[Ni(o\text{-HOdtb})(o\text{-HOdtbS})]$	Purple	95	88	13.3 (13.7)	38.1 (37.3)	38.1 (39.2)	2.1 (2.3)	—	Dia	428
$[Cu(o\text{-Odtb})]$	Brown	120–121	85	26.6 (27.4)	28.2 (27.6)	36.1 (36.3)	1.5 (1.7)	—	1.7	460
$[Bu^n_4N][Zn(o\text{-HOdtb})_3]$	Orange	92	81	8.3 (8.0)	23.2 (23.6)	54.5 (54.5)	6.0 (6.2)	1.6 (1.7)	Dia	—

and antitumor activity of transition metal complexes of *o*-hydroxydithiobenzoate. Further, we also investigated the immunomodulatory action of these complexes in a tumor bearing host.

Results and Discussion

The binary complexes of *o*-hydroxydithiobenzoate are soluble in common organic solvents such as chloroform, ethanol, acetone, DMSO and melt in the range of 88–139 °C. $H_2C(o\text{-HOdtb})_2$ formed by the reaction of $[Bu^n_4N][Zn(o\text{-HOdtb})_3]$ and CH_2Cl_2 is not metal assisted because $[Bu^n_4N][o\text{-HOdtb})]$ when crystallized in CH_2Cl_2 gave yellow crystalline solid which showed spectra identical to the spectra of $H_2C(o\text{-HOdtb})_2$. The composition of the complexes along with colour, mp, magnetic susceptibility and elemental analyses are given in Table 1.

Magnetic properties and electronic spectra

[Ni(*o*-HOdtb)(*o*-HOdtbS)] is diamagnetic and its UV–visible spectrum shows a very intense band at 526 (ε 825) nm, characteristic of dithio-perthiocarboxylato nickel(II) with a shoulder at 430 (ε 1550) nm assigned to the $^1A_{1g}\rightarrow{}^1B_{3g}$ and metal to ligand charge-transfer transitions, respectively. Other bands at 368 (ε 2050), 328 (ε 6800) and 288 (ε 3600) nm have been assigned to possible intra-ligand transitions. The magnetic and spectral behavior suggests a square planar geometry, as reported for other dithio-perthiocarboxalyto nickel(II) complexes, containing a basically square planar low-spin $[NiS_4]$ chromophore. The spectrum of the four coordinate, dimeric [Cu(*o*-Odtb)] shows bands at 968 (ε 200), 910 (ε 600) and 816 (ε 900) nm typical of distorted tetrahedral copper(II), the usual distortion being the flattening of the tetrahedron along a 2-fold axis resulting in a structure of D_{2d} symmetry which would retain the degeneracy of xy, yz and lead to three possible transitions, namely from the ground state $^2B_2$ to ^2E, $^2B_1$ and $^2A_1$,[15] other bands at 459 (ε 2100) and 380 (ε 4600) nm are assigned to charge-transfer transitions, and the band at 300 (ε 5100) nm was due to the ligand transition. [Co(*o*-HOdtb)$_3$] shows a band at 452 (ε 624) nm assigned to the $^1A_1g\rightarrow{}^1T_2g$ transition and the bands at 380 (ε 2960) and 312 (ε 5200) nm are attributed to the metal–ligand

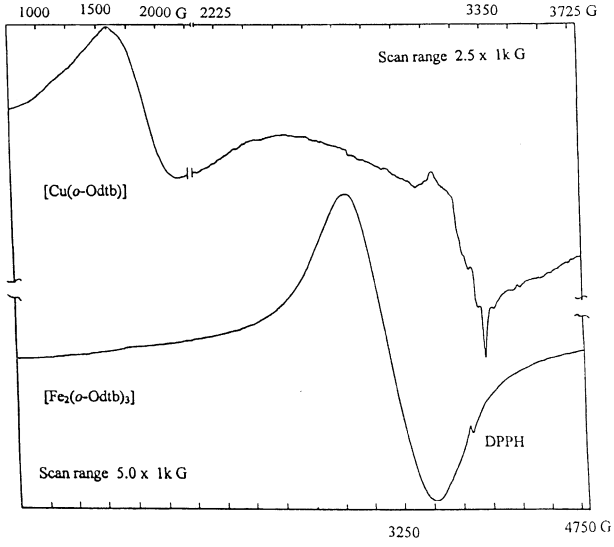

Figure 1. Solid-state ESR spectra of [Cu(*o*-Odtb)] and [Fe_2(*o*-Odtb)$_3$] at 298 K.

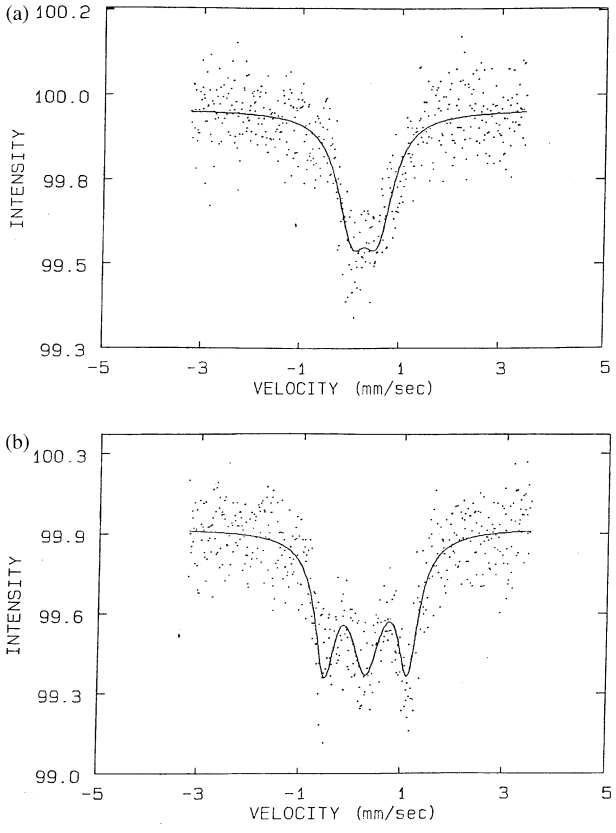

Figure 2. (a) Mössbauer spectrum of [Fe_2(*o*-Odtb)$_3$] at room temperature; (b) Mössbauer spectrum of [Fe_2(*o*-Odtb)$_3$] at 78 K.

and intra–ligand transitions, respectively, for an octahedral Co(III). [Fe_2(*o*-Odtb)$_3$] exhibits a magnetic moment of 5.9 BM for high-spin iron(III) centre. The electronic spectrum displays a band at 468 (ε 3560) nm assigned to the charge transfer transition and the geometry assigned around Fe(III) is assumed to be octahedral.[16]

IR spectra

The IR spectrum of the ligand displays bands at 3450 and 1379 cm^{-1} which are assigned to the stretching and in-plane bending modes of the –OH group. These modes absorb in the regions of 3398–3315 and 1400–1360 cm^{-1}, respectively, in the complexes, indicating that the –OH group of the *o*-hydroxydithiobenzoate is not involved in bond formation with Zn(II) and Ni(II) but its appearance at higher frequency suggests the presence of intramolecular hydrogen bonding in the free ligand which is broken on complex formation.[17] The phenyl carbon stretching frequency occurs between 1236 and 1285 cm^{-1} in all the complexes. The decrease in this frequency parallels the decrease in the affinity of the metal ion for sulfur.[18] All the carbon–sulfur stretching frequencies occur between 900 and 1100 cm^{-1} and the geometry around the metal atom has little effect on this frequency. Two bands are observed at ca. 970–1035 cm^{-1} in the spectra of all the complexes for ν_{sym} (C–S) and ν_{as} (C–S) modes, respectively, except for the Ni(II) complex. The spectrum of [Ni(*o*-HOdtb)(*o*-HOdtbS)], however, shows four bands at 1000, 985, 960 and 920 cm^{-1}. As the chelate ring is expanded by the addition of a sulfur atom, four stretching modes should be found, two due to the four membered ring and two due to the five-membered ring.[19] Thus, by comparison with the spectra of other complexes, the two bands at 985 and 1000 cm^{-1} are attributed to the four-membered ring and the remaining two at 960 and 920 cm^{-1} to the five-membered ring in [Ni(*o*-HOdtb)(*o*-HOdtbS)]. The IR spectra of the complexes show that the ligand is bonded to the metal ion as a uninegative, bonding through sulfur atoms in [Ni(*o*-HOdtb)(*o*-HOdtbS)], [Co(*o*-HOdtb)$_3$], and [Bu^n_4N][Zn(*o*-HOdtb)$_3$], whereas, the ligand acts as a binegative bonding through both sulfur and oxygen in [Cu(*o*-Odtb)], [Fe_2 (*o*-HOdtb)$_3$], and [Bu^n_4N][V(*o*-Odtb)$_3$].

ESR spectra

The ESR spectrum (Fig. 1) of [Fe_2(*o*-Odtb)$_3$] in the solid state shows a broad signal with $<g>$ value of 2.08 as observed for octahedral iron(III) complexes. The spectrum of Cu(*o*-Odtb) shows three separate signals in the high-field region with $g_z = 2.60$, $g_y = 2.17$ and $g_x = 2.01$. In addition, the presence of a broad signal at 1785 G indicates that the compound is dimeric.[20]

Mössbauer spectrum

The room temperature Mössbauer spectrum (Fig. 2a) of [Fe_2(*o*-Odtb)$_3$] shows a doublet with an isomer shift of $\delta = 0.32\ mm\ s^{-1}$ and quadrupole splitting of $\Delta Eq = 0.51\ mm\ s^{-1}$ and suggests the presence of high-spin ($S = 5/2$) ground state for iron(III).[21] The spectrum (Fig. 2b) of the complex shows a triplet at liquid nitrogen temperature characteristic of a low symmetry iron(III)

Table 2. Selected interatomic distances (Å)

Atom1	Atom2	Distance	Atom1	Atom2	Distance
a. Within [Zn(*o*-HOdtb)$_3$]					
Zn	S1	2.4386(8)	C11	C16	1.425(5)
Zn	S2	2.5078(8)	C12	C13	1.404(5)
Zn	S3	2.3063(8)	C13	C14	1.350(6)
Zn	S4	2.9712(8)[a]	C14	C15	1.370(6)
Zn	S5	2.2986(8)	C15	C16	1.360(5)
Zn	S6	3.1231(8)[a]	C20	C21	1.466(4)
S1	C10	1.711(3)	C21	C22	1.417(4)
S2	C10	1.701(3)	C21	C26	1.411(4)
S2	H10	2.15[a]	C22	C23	1.412(4)
S3	C20	1.724(3)	C23	C24	1.368(5)
S4	C20	1.682(3)	C24	C25	1.390(5)
S4	H20	2.18[a]	C25	C26	1.369(4)
S5	C30	1.725(3)	C30	C31	1.486(4)
S6	C30	1.673(3)	C31	C32	1.415(4)
S6	H30	2.14[a]	C31	C36	1.403(4)
O1	C12	1.320(5)	C32	C33	1.394(4)
O2	C22	1.337(4)	C33	C34	1.355(5)
O3	C32	1.351(4)	C34	C35	1.395(5)
C10	C11	1.465(4)	C35	C36	1.361(4)
C11	C12	1.405(5)			
b. Within the tetra-*n*-butylammonium ion					
N	C40	1.530(4)	C45	C46	1.528(4)
N	C44	1.527(4)	C46	C47	1.520(4)
N	C48	1.527(4)	C48	C49	1.520(4)
N	C52	1.521(4)	C49	C50	1.530(5)
C40	C41	1.523(4)	C50	C51	1.431(6)
C41	C42	1.527(4)	C52	C53	1.504(4)
C42	C43	1.517(5)	C53	C54	1.525(4)
C44	C45	1.512(4)	C54	C55	1.517(5)

[a]Non-bonded distance.

complex. The Mössbauer parameters are: isomer shift $\delta = 0.30\,mm\,s^{-1}$ and quadrupole splitting $\Delta Eq = 1.66\,mm\,s^{-1}$ for site one and the corresponding values for site two are $\delta = 0.29\,mm\,s^{-1}$ and $\Delta Eq = 0$.

Single crystal X-ray diffraction analysis of $[Bu^n_4N][Zn(o\text{-HOdtb})_3]$ and $H_2C(o\text{-HOdtb})_2$

A crystal of *n*-tetrabutylammonium tris(*o*-hydroxydithiobenzoato)zincate(II) and $H_2C(o\text{-HOdtb})_2$, were

Table 3. Selected interatomic angles (°)

Atom1	Atom2	Atom3	Angle	Atom1	Atom2	Atom3	Angle
a. Within [Zn(*o*-HOdtb)$_3$]							
S1	Zn	S2	71.41(3)	S4	C20	C21	123.7(2)
S1	Zn	S3	105.78(3)	C20	C21	C22	123.7(3)
S1	Zn	S5	114.52(3)	C20	C21	C26	120.3(2)
S2	Zn	S3	102.71(3)	C22	C21	C26	116.0(2)
S2	Zn	S5	113.56(3)	O2	C22	C21	124.8(3)
S3	Zn	S5	132.14(3)	O2	C22	C23	115.5(3)
Zn	S1	C10	87.02(10)	C21	C22	C23	119.7(3)
Zn	S2	C10	85.01(10)	C22	C23	C24	121.8(3)
Zn	S3	C20	97.73(10)	C23	C24	C25	119.4(3)
Zn	S5	C30	100.45(10)	C24	C25	C26	119.5(3)
S1	C10	S2	115.66(16)	C21	C26	C25	123.6(3)
S1	C10	C11	121.2(2)	S5	C30	S6	119.37(17)
S2	C10	C11	123.1(2)	S5	C30	C31	117.1(2)
C10	C11	C12	123.7(3)	S6	C30	C31	123.6(2)
C10	C11	C16	119.9(3)	C30	C31	C32	123.5(3)
C12	C11	C16	116.2(3)	C30	C31	C36	120.6(2)
O1	C12	C11	126.9(3)	C32	C31	C36	115.8(3)
O1	C12	C13	113.2(3)	O3	C32	C31	124.2(3)
C11	C12	C13	119.9(3)	O3	C32	C33	115.5(3)
C12	C13	C14	121.1(4)	C31	C32	C33	120.3(3)
C13	C14	C15	120.6(4)	C32	C33	C34	121.3(3)
C14	C15	C16	120.0(4)	C33	C34	C35	120.0(3)
C11	C16	C15	122.1(4)	C34	C35	C36	118.9(3)
S3	C20	S4	118.57(16)	C31	C36	C35	123.7(3)
S3	C20	C21	117.7(2)				
b. Within the tetra-*n*-butylammonium ion							
C40	N	C44	110.8(2)	N	C44	C45	115.0(2)
C40	N	C48	108.9(2)	C44	C45	C46	110.5(2)
C40	N	C52	108.3(2)	C45	C46	C47	113.4(3)
C44	N	C48	108.2(2)	N	C48	C49	116.4(2)
C44	N	C52	109.3(2)	C48	C49	C50	110.3(3)
C48	N	C52	111.3(2)	C49	C50	C51	117.1(4)
N	C40	C41	113.9(2)	N	C52	C53	116.2(2)
C40	C41	C42	111.3(3)	C52	C53	C54	108.7(3)
C41	C42	C43	112.0(3)	C53	C54	C55	112.5(3)

Table 4. Selected interatomic distances (Å)

Atom1	Atom2	Distance	Atom1	Atom2	Distance
S1	C7	1.756(3)	C1	C6	1.407(4)
S1	C8	1.800(2)	C1	C7	1.468(4)
S2	C7	1.661(3)	C2	C3	1.394(4)
S2	H10	2.14[a]	C3	C4	1.362(5)
O	C2	1.345(3)	C4	C5	1.391(4)
C1	C2	1.416(4)	C5	C6	1.376(4)

[a]Non-bonded distance.

Table 5. Selected interatomic angles (°)

Atom1	Atom2	Atom3	Angle	Atom1	Atom2	Atom3	Angle
C7	S1	C8	103.14(9)	C3	C4	C5	119.9(3)
C2	C1	C6	116.7(2)	C4	C5	C6	119.5(3)
C2	C1	C7	123.3(2)	C1	C6	C5	122.4(3)
C6	C1	C7	120.0(2)	S1	C7	S2	120.69(16)
O	C2	C1	124.6(3)	S1	C7	C1	113.84(18)
O	C2	C3	115.4(2)	S2	C7	C1	125.44(19)
C1	C2	C3	120.0(2)	S1	C8	S1′	116.6(2)
C2	C3	C4	121.5(3)				

obtained from slow evaporation of the solution of the compound in acetone and dichloromethane, respectively, at room temperature. The crystal data, selected interatomic distances, selected interatomic angles and atomic coordinates are given in Tables 2–5. The structures are illustrated in Figure 3a and b. The structure of $[Bu^n_4N][Zn(o\text{-}HOdtb)_3]$ shows that one *o*-hydroxydithiobenzoato ligand is conventionally bidentate (Zn–S 2.43 and 2.50 Å) whereas the other two ligands are formally unidentate, with a mean Zn–S distance of 2.30 Å, while the non-bonded Zn–S contacts have a mean value of 3.04 Å. The coordination geometry of the zinc atom is distorted tetrahedral (or distorted trigonal prismatic if all sulfur atoms are considered to be bonded). The Zn–S contact of this magnitude (van der Waals distance is 3.27 Å) a necessary consequence of intramolecular rotational constraints, there being available intramolecular rotational pathways which would ease undesirable interaction at negligible cost to the potential energy of the system. It may therefore be concluded that a weak bonding interaction between zinc and sulfur occurs in the complex. The structure reveal, unexpectedly, that atleast two of the potentially chelating ligands are only weakly bidentate with respect to zinc.[22] The structure of $H_2C(o\text{-}HOdtb)_2$ reveals that there exists hydrogen bonding between hydroxyl proton and sulfur of the same dithiobenzoate which stabilizes the tetrahedral structure.

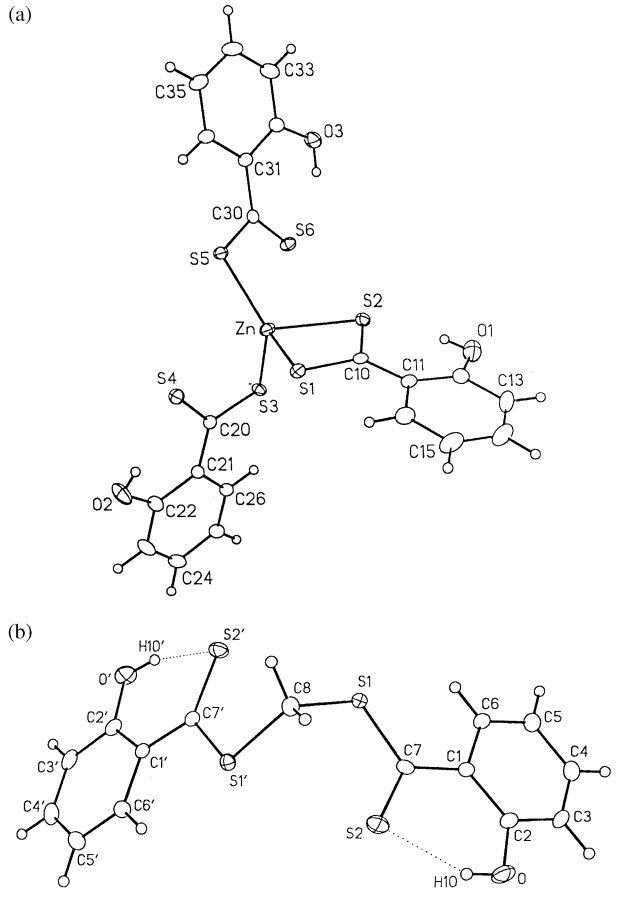

Figure 3. (a) Perspective view of the $[Zn(o\text{-}HOdtb)_3]^-$ complex anion showing the atom labeling scheme. Non-hydrogen atoms are represented by Gaussian ellipsoids at the 20% probability level. Hydrogen atoms are shown with arbitrarily small thermal parameters. (b) Perspective view of the $H_2C(o\text{-}HOdtb)_2$ showing atomic labeling scheme.

Antitumor activity. In vitro and in vivo antitumor activity was assayed in order to test the cytotoxic properties of the ligand and its metal complexes. As indicated by the data presented in the (Table 6), all the complexes have a pronounced inhibitory effect on DNA synthesis. It is also evident from the data that complexation of the ligand with metal ions further enhances the inhibition of DNA synthesis. The ligand alone was found to cause insignificant inhibition, whereas, its metal complexes caused maximum inhibition. Among the metal complexes, [Ni(*o*-HOdtb)(*o*-HOdtbS)], [Cu(*o*-Odtb)], [Fe_2

Table 6. Percentage inhibition of ^{3}H-thymidine incorporation

Compound	% Inhibition	
	1 μg cm^{-3}	5 μg cm^{-3}
Na(*o*-HOdtb)	26.2	28.2
[Ni(*o*-HOdtb)(*o*-HOdtbS)]	88.6	87.3
[Cu(*o*-Odtb)]	78.6	83.2
$[Fe_2(o\text{-}Odtb)_3]$	75.1	85.8
$[Co(o\text{-}OHdtb)_3]$	72.9	81.9
$[Bu^n_4N][V(o\text{-}Odtb)_3]$	54.8	55.1
$[Bu^n_4N][Zn(o\text{-}HOdtb)_3]$	53.9	61.8
Cisplatin	85.6	80.3

Table 7. Effect of $[Bu^n_4N][o\text{-}HOdtb]$ and its metal complexes on tumor cell growth in vitro (ID_{50} values in μg/mL)

Compound	ID_{50} (μg/mL)
$[Bu^n_4N][o\text{-}HOdtb]$	18.60
[Na(*o*-HOdtb)]	17.80
[Ni(*o*-HOdtb)(*o*-HOdtbS)]	0.88
[Cu(*o*-Odtb)]	0.92
$[Fe_2(o\text{-}Odtb)_3]$	1.10
$[Co(o\text{-}HOdtb)_3]$	1.63
$[Bu^n_4N][V(o\text{-}Odtb)_3]$	1.83
$[Bu^n_4N][Zn(o\text{-}HOdtb)_3]$	1.80
Cisplatin	0.73

ID_{50}, average drug concentration (μg/mL) for 50% inhibition of Dalton's Lymphoma growth. Values are mean ± SD of three experiments. $\rho < 0.05$ with respect to values of ID_{50} of ligand alone.

Table 8. Responses of DL inoculated mice to a single treatment with Na(*o*-OHdtb), Bu^n_4N(*o*-OHdtb) and their transition metal complex

Compound	Post inoculation life span (% T/C)
$[Bu^n_4N][o\text{-}HOdtb]$	102
[Na(*o*-HOdtb)]	112
[Ni(*o*-HOdtb)(*o*-HOdtbS]	260
[Cu(*o*-Odtb)]	255
$[Fe_2(o\text{-}Odtb)_3]$	245
$[Co(o\text{-}HOdtb)_3]$	180
$[Bu^n_4N][V(o\text{-}Odtb)_3]$	160
$[Bu^n_4N][Zn(o\text{-}HOdtb)_3]$	153
Cisplatin	250

All the solutions were delivered ip (10 mg/kg). Solutions prepared were 10 mg/10 mL in ethanol. Control mice were injected with 10 mL of ethanol per kg wt of mouse. Treatment responses (six mice per treatment group) presented as % T/C, was calculated according to the equation: mean life span of treated mice/mean life span of control mice by 100. A % T/C > 125 is considered biologically significant. C = 20 days, experiment terminated after 50 days.

(o-Odtb)$_3$], [Co(o-HOdtb)$_3$] showed maximum inhibitory effect, whereas [Bu^n_4N][V(o-Odtb)$_3$]) and [Bu^n_4N][Zn(o-HOdtb)$_3$] showed relatively less effect on DNA synthesis. Percentage inhibition of thymidine incorporation was studied at a dose of 1 and 5 μg/mL. On increasing the dose from 1 to 5 μg/mL, the percentage inhibition of thymidine incorporation increases, except for [Ni(o-HOdtb)(o-HOdtbS)] where there is a decrease in percentage inhibition of ^{3}H-thymidine incorporation. The reason for the observed inhibition of DNA blastogenesis by the metal complexes is unclear however, several possibilities could be considered. The inhibition in tumor cell blastogenesis could be a direct result of the interaction of the metal complexes with DNA, which interfere with the

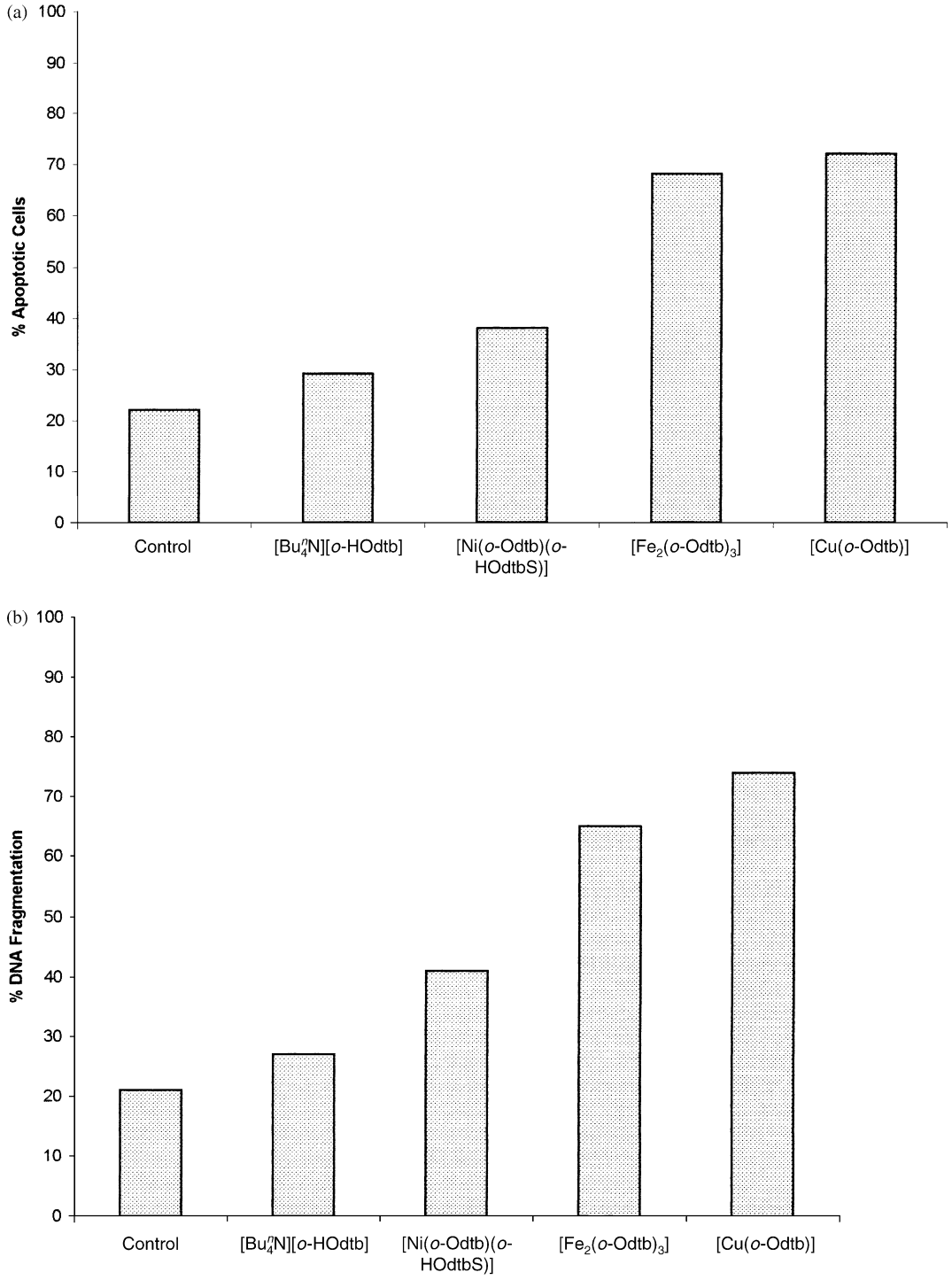

Figure 4. (a) Effect of ligand and its metal complexes on the induction of apoptosis in tumor cells. DL cells were incubated in medium alone or containing ligand or its metal complexes (10 mg/mL) for 24 h and the number of cells showing apoptotic morphology was enumerated. Values are mean of three experiments. (b) Effect of [Bu^n_4N][o-HOdtbh] and its metal complexes on % DNA fragmentation of tumor cells. DL cells were incubated in medium alone or containing [Bu^n_4N][o-HOdtbh] or its metal complexes (10 μg/mL) for 24 h and the % DNA fragmentation was evaluated. Values are mean of three experiments.

normal process of its replication. Indeed, DNA binding of metal complexes of sulfur donor ligands has been documented.[23] Furthermore, inhibition/activation of various enzymes directly/indirectly involved in DNA replication is not ruled out. Interaction of metal complexes with protein components of viable cells has been reported.[24,25] Binding of metal complexes with protein may cause alterations in the domain organization of protein probably in a similar manner as the one observed in case of allosteric enzymes leading to their malfunctioning. However, more studies will be needed to confirm existence of one or more of such possibilities in our system. One of the additional supporting evidence comes from the result of experiments in which tumor cells, incubated in the presence or absence of metal complexes were checked for their effect on viability by MTT assay in which 3,(4,5-dimethylthiazol-2-yl)-2,5-diphenyl tetrazolium bromide) is metabolized to an insoluble colored formazan salt by mitochondrial enzyme activity of succinate dehydrogenase in living cells.[26] The growth inhibitory effects of

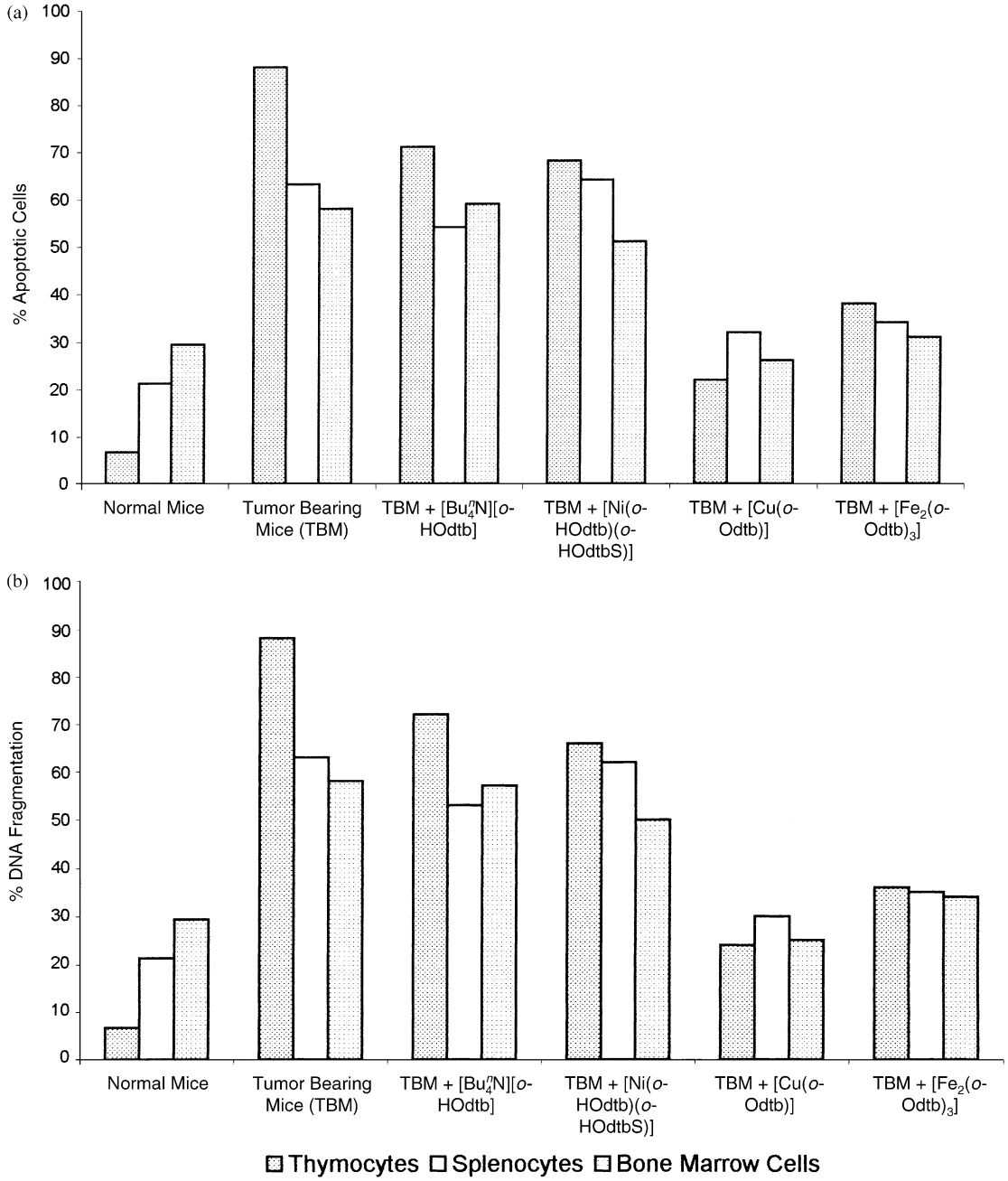

Figure 5. (a) Effect of in vitro administration of ligand or its metal complexes on the induction of apoptosis in thymocyte, splenocyte and bone marrow cell of normal or tumor-bearing mice treated with ligand or its metal complexes. Thymocytes, splenocytes and bone marrow cells of normal or tumor-bearing mice treated with ligand or its metal complexes were enumerated for the number of cell showing apoptotic morphology. Values are mean of three experiments. (b) Effect of in vivo administration of ligand or itsmetal complexes on % DNA fragmentation of thymocyte, splenocyte and bone marrow cell of normal or tumor-bearing mice with ligand or its metal complexes. Thymocytes, splenocytes and bone marrow cells of normal or tumor-bearing mice or tumor-bearing mice treated with ligand or its metal complexes and checked for % DNA fragmentation. Values are mean of three experiments.

these complexes in terms of ID_{50} values were studied (Table 7) against murine tumor cell line. All the complexes display significant inhibitory effect on proliferation of tumor cell in vitro. [Ni(*o*-HOdtb)(*o*-HOdtbS)], [Cu(*o*-Odtb)] and [Fe_2(*o*-Odtb)$_3$] were found to possess significant inhibitory effect on tumor cell proliferation. However, the ligand alone failed to cause significant inhibitory action on tumor cell proliferation as is evident from its high ID_{50} value.

In the next part of the investigation we studied the effect of the metal complexes on tumor cell killing to identify the mode of cell death. The results suggest that apoptosis induced in tumor cells treated with [Cu(*o*Odtb)] and [Fe_2(*o*-Odtb)$_3$] were found to be most effective in the induction of tumor cell apoptosis (Fig. 4a). The mechanism of the induction of apoptosis remains poorly understood and is thought to be dependent on multiple mechanism(s) ultimately culminating in the activation of DNA cleaving endonucleases.[27] Indeed, results presented in Figure 4b show that [Cu(*o*Odtb)] and [Fe_2 (*o*-Odtb)$_3$] cause an increase in the percentage of specific DNA fragmentation, a hallmark feature of apoptosis, indicating that these metal complexes may induce apoptosis culminating in the activation of endonucleases causing DNA fragmentation.

Furthermore, the metal complexes at the concentration checked did not inhibit the proliferation of normal splenocyte and bone marrow cells (data not shown), indicating that the cytostatic effect of the metal complexes was restricted to the tumor phenotype alone. Selective killing of tumor cells could be attributed to the fact that tumor cells are unable to counter the load of mutations owing to their defective DNA repair mechanism.[28]

In the next part of the investigation, we checked the life prolonging effect in Dalton's Lymphoma (DL) bearing mice administered with PBS (phosphate buffer saline) alone or containing the ligand or the metal complexes as indicated in the Experimental. As shown in Table 8, minimal % T/C was observed in mice administered with ligand alone as compared to that of mice administered with metal complexes. Maximum % T/C was found for [Ni(*o*-HOdtb)(*o*-HOdtbS)], [Cu(*o*-Odtb)], [Fe_2(*o*-Odtb)$_3$] as compared to [Co(*o*-HOdtb)$_3$], [Bu^n_4N][V(*o*-Odtb)$_3$] and [Bu^n_4N][Zn(*o*-HOdtb)$_3$]. Increase in the value of % T/C indicates a prolongation of the life of tumor bearing mice and suggests that such effect could either result from the direct cytotoxic/cytostatic action of the complexes on tumor cells or due to the activation of certain host derived antitumor defense mechanism(s).

Progression of growth of various tumors including DL is invariably associated with the onset of immunosuppression in tumor-bearing host[29–32] one of the reasons being induction of apoptosis and inhibition of proliferation of hematopoietic precursor cells.[33,34] Since in vivo administration of these metal complexes prolonged survival of tumor bearing animals and these metal complexes did not show cytotoxicity against normal cells in vitro, we were interested to investigate if the administration of metal complexes could reverse tumor growth associated induction of apoptosis in various hematopoietic cells. For this, tumor (DL) bearing mice were administered with metal complexes, and the % of

Table 9. Crystallographic experimental details

Crystal data		
Formula	$C_{37}H_{51}NO_3S_6Zn$	$C_{15}H_{12}O_2S_4$
Formula weight	815.52	352.49
Crystal dimensions (mm)	0.34×0.33×0.18	0.54×0.17×0.09
Crystal system	Orthorhombic	Monoclinic
Space group	$Pna2_1$ (no. 33)	C2 (no. 5)
Unit cell parameters		
a (Å)	20.8193(11)	12.9036(14)
b (Å)	9.0332(5)	4.1402(4)
c (Å)	21.1415(10)	14.2005(16)
V (Å^3)	3976.0(4)	747.71(14)
Z	4	2
ρ_{calcd} (g cm^{-3})	1.362	1.566
μ (mm^{-1})	1.362	0.635
Data collection and refinement conditions		
Diffractometer	Bruker P4/RA/SMART 1000 CCD[37]	
Radiation [λ(Å)]	Graphite-monochromated Mo K_α(0.71073)	
Temperature (°C)	−80	−80
Scan type	ϕ rotations (0.3°)/ω scans (0.3°) (20 s exposure)	
Data collection 2θ limit (°)	52.90	52.68
Total data collected	20,632 ($-26\le h\le 25$, $-10\le k\le 11$, $-22\le l\le 26$); 1861($-16\le h\le 14$, $-5\le k\le 2$, $-17\le l\le 17$)	
Independent reflections	7036	1106
Number of observations (NO)	6308 [$Fo^2\ge 2\sigma(Fo^2)$]	1022[$Fo^2\ge 2\sigma(Fo^2)$]
Structure solution method	Direct methods (*SHELXS*-86[38])	
Refinement method	Full matrix least-squares on F^2 (*SHELXL*-93[39])	
Absorption correction method	SADABS	
Range of transmission factors	0.8620–0.6174	0.9562–0.4844
Data/restraints/parameters	7036[$Fo^2\ge -3\sigma(Fo^2)$]/0/436	1106[$Fo^2\ge -3\sigma(Fo^2)$]/0/67
Flack absolute structure parameter[40]	0.024(9)	0.11(13)
Goodness-of-fit (*S*)	0.995[$Fo^2\ge -3\sigma(Fo^2)$]	1.077[$Fo^2\ge -3\sigma(Fo^2)$]

apoptotic thymocyte, splenocyte and bone marrow cells were enumerated. As shown in Figure 5a, administration of metal complexes in tumor bearing mice resulted in the inhibition of tumor associated apoptosis of thymocyte, splenocyte and bone marrow cells. Similar results were obtained for % DNA fragmentation as well (Fig. 5b). The reversal of tumor growth associated induction of apoptosis of hematopoietic cells by metal complexes is predicted to be due to two reasons: (i) reduction of tumor load resulting due to the cytotoxic effect of metal complexes on tumor cells, leading to a decrease in the tumor associated concentration of apoptotic factors; (ii) direct protective effect of metal complexes on the hematopoietic cells. Although not very clear, the probability of the latter could be due to the fact that metal complexes can bind to DNA and several proteins in cells, which could result in the protective effect.

Conclusions

Although more investigations will be required to confirm the mechanism of action of metal complexes on tumor and normal cells, the study suggests that [Cu(*o*-Odtb)] and [Fe_2(*o*-Odtb)$_3$] can cause prolongation of survival in tumor bearing animals by:

1. Directly killing tumor cells.
2. Reversing tumor associated immunosuppression.

The finding of this investigation may have long lasting clinical implication with the novel proposition that metal complexes of *o*-hydroxydithiobenzoate may have dual mechanism of action in tumor regression. Many anticancer drugs in use are cell-cycle specific.[35] The inactivity of the ligand against tumor cells could be due to lack of cell-cycle specificity towards their activity and to a reversible nature of their interactions with cells. The importance of such work lies in the possibility that the new complexes might be more efficacious drugs against tumors for which a thorough investigation regarding the structure–activity of the complexes and their stability is required in order to understand the variation in their biological effects, which could be helpful in designing more potent antitumor agents for therapeutic use.

Experimental

Physical measurements

Melting points (uncorrected) were determined in a Thomas-Hoover capillary melting point apparatus. Elemental analyses (C,H,N) were performed on a Perkin-Elmer 240C model microanalyzer. All the complexes were analyzed for their metal content, following standard procedures.[36] Sulfur was estimated as $BaSO_4$. Magnetic susceptibility measurements were made at room temperature on a Cahn–Faraday balance using $Hg[Co(NCS)_4]$ as calibrant. Electronic spectra were recorded on CARY-2390 UV–visible spectrophotometer in $CHCl_3$. Infrared spectra were recorded as KBr pellets in the region 4000–400 cm^{-1} on a Jasco FT/IR-5300 spectrophotometer. Proton magnetic resonance (^{1}H NMR) spectra were recorded on a 90 MHz Jeol FX-90Q spectrometer. The chemical shift values are expressed as δ values (parts per million) relative to tetramethylsilane as an internal standard. Esr spectra were recorded on a X-band spectrometer model EPR-112 using DDPH as a 'g' marker. The Mössbauer spectra were collected using a cryophysics MS-1 microprocessor-controlled spectrometer operating in the constant acceleration mode. The source was 25 mci-^{57}Co/Rh and spectra were fitted using a standard non-linear least square package. The FAB mass spectra were recorded on a Jeol SX 102/DA-6000 mass spectrometer/Data system using Argon/ Xenon (6 KV, 10 mA) as the FAB gas and *m*-nitrobenzyl alcohol (NBA) as a matrix. X-ray diffraction analysis was carried out on Bruker diffractometer. Crystallographic experimental details are given in Table 9.[37–40]

Antitumor screening

Mice. Inbred populations of BALB/c mice of either sex of 8–12 weeks were used for the study. The mice were fed food and water ad libitum under pathogen-free conditions and were treated with utmost human care.

Tumor systems. Dalton's lymphoma (a spontaneous murine T cell lymphoma) were maintained in culture in vitro as well as in ascites by serial transplantation in BALB/c mice by an intraperitoneal injection of 5×10^5 cells/mouse.

Thymocyte preparation and culture. Thymuses obtained from normal and tumor bearing mice with or without administration of complexes were weighed on a chilled watch glass, diced on ice and passed through a stainless steel screen using a syringe plunger. These cells, after washing with phosphate buffered saline (PBS) by centrifugation at 200*g* for 10 min at 4 °C, were used directly for thymocyte counts. Cell viability in the thymocyte preparation was determined by mixing 10 mL sample with an equal volume of 0.4% trypan blue–PBS solution[41] and counting the cells on a hemocytometer under light microscope. Cells that did not excude trypan blue were considered nonviable. For culturing thymocytes in vitro, thymocytes were maintained in complete RPMI 1640 medium at 37 °C in humidified atmosphere of 5% CO_2 in air.

Splenocyte preparation and culture. Spleens obtained from normal and tumor bearing mice with or without administration of complexes were weighed on a chilled watch glass, diced on ice and passed through a stainless steel screen using a syringe plunger. These cells, after washing with phosphate buffered saline (PBS) by centrifugation at 200*g* for 10 min at 4 °C, RBC were depleted by treatment with 0.84% ammonium chloride for 10 min at room temperature. Cells were again washed in PBS and then cultured in a humidified atmosphere at 5% CO_2, to remove adherent cells. Non-adherent cells were collected and used for assay.

Bone marrow cell preparation and culture. Bone marrow cells (BMC) were obtained from the femurs of normal

and tumor bearing mice with or without administration of complexes, as described elsewhere.[42] Briefly, the mice were killed by cervical dislocation and the BMC were obtained from the femoral shafts by flushing it with serum-free medium. BMC were then agitated gently to prepare a single cell suspension and then washed thrice with serum-free medium by centrifugation at 200*g* at 4 °C. BMC were then incubated in plastic tissue culture flask for 2 h at 37 °C to remove the adherent macrophage. The non adherent BMC were then used for proliferation.

Proliferation assay

Different cells obtained from normal or tumor bearing mice treated with or without complexes were incubated at a concentration of 1.5×10^6 cells per well in a 96-well plastic tissue culture plate with medium containing submitogenic doses of concanavalin-A (1 μg/mL). Cultures were then incubated at 37 °C in CO_2 incubator for 48 h and assayed for proliferation and growth inhibition using MTT assay. It was used to measure the cytotoxic effect of the ligand and the complexes. The procedures employed the pale yellow tetrazolium salt [3-(4,5-dimethylthiazol)-2-yl-2,5-diphenyl-2H-tetrazolium bromide] (MTT), which was cleaved by active mitochondria to form a dark blue formazon product that can be completely solubilized in acidic isopropanol.[43] The assay provides a simple way to detect living and growing cells without use of radioactivity. Briefly, 5×10^4 tumor cells were plated in triplicate in 96-well flat-bottom tissue culture plates, and treated with different concentrations of drugs for the time indicated. MTT (0.005 g cm^{-3} in PBS) was added to the cell culture and incubated for 4 h in a 37 °C, 5% CO_2 humidified incubator. The formazon crystals formed during the reaction were dissolved in 100 mL of 0.04 N HCl in isopropanol and absorbance was read at 570 nm. The average drug concentration (μg/mL) for 50% inhibition (ID_{50}) of tumor-cell growth was determined by plotting the log of drug concentration versus the growth rate (% control).

Morphological evaluation of apoptotic cells. Cells were air dried, fixed in methanol, stained with Wright staining solution, mounted in glycerine and analyzed under light microscope at 45× magnification. Apoptotic cells were identified on the basis of morphological features that included contracted cell bodies, condensed, uniformly circumscribed and densely stained chromatin, or membrane-bound apoptotic bodies containing one or more nuclear fragments.[44] The percentage of apoptotic cells was determined by counting more than 300 cells in at least three separate visions.

Quantitation of percent DNA fragmentation

Percent DNA fragmentation was quantified following a method described by Sellins and Cohen[45] with slight modification. Cells (5×10^5 cells/mL) were suspended in 0.5 mL of lysis buffer (Tris—EDTA buffer, pH 7.4 containing 0.2% Trinton X-100) and were centrifuged for 15 min at 13,000*g* at 4 °C in a microfuge tube (labeled as B). Supernatant was transferred to another tube (labeled as T). 0.5 mL of 25% trichloroacetic acid was added to T and B tubes, which were then vortexed vigorously. Tubes were kept overnight at 4 °C for precipitation. Supernatant was discarded after centrifugation at 13,000*g* for 10 min and then DNA in each pellet was hydrolyzed with 80 μL of 5% trichloroacetic acid by heating on water bath at 90 °C for 15 min and 160 μL of freshly prepared diphenylamine (150 mg diphenylamine in 10 mL glacial acetic acid, 150 μL concd H_2SO_4 and 50 mL of acetaldehyde solution) was added and the tubes were allowed to stand overnight at room temperature to develop color. 100 μL of this colored solution was transferred to a 96-well flat-bottom ELISA plate (NUNC, Denmark) and absorbance at 600 nm noted on an ELISA plate reader (BioRad, Australia). Percent fragmented DNA was calculated using formula:

$$\%\ \text{fragmented DNA} = \frac{T}{T+B}100$$

where T = absorbance of fragmented DNA, T + B = absorbance of total DNA.

In vivo studies

In order to aassess the antitumor activity of the compounds, 6–8 groups of BALB/c mice were inoculated intraperitoneally with DL (10^6) cells followed by treatment with the metal complexes (10 mg/kg body weight) in a single ip injection on days 1, 5, 9 and 12 after tumor transplantation. This treatment protocol was selected for administration, as various previous studies[46] have shown that metal complexes of sulfur donor ligands have shown optimal antitumor activity at a dose of 10 mg/kg.The antitumor efficacy of each agent is expressed as% T/C and is given by,

$$\%\ \text{TC} = \frac{\text{Mean life span of treated mice}}{\text{Mean life span of control mice}} \times 100$$

In vitro DNA synthesis inhibition assay

The DL cell suspensions were prepared in a complete medium (RPMI 1640 medium supplemented with penicillin, streptomycin and 10% heat-inactivated fetal calf serum) at a concentration of 10^6 cells /mL. 2×10^5 cells per well were added to duplicate wells of a 96-well plate (NUNC, Denmark). The cells were treated with the test compounds at various doses (1 and 5 μg/mL) and incubated for 24 h at 37 °C in a CO_2 incubator. In control sets no treatment was given. After 24 h of incubation, the cells were washed 3× with RPMI 1640 culture medium (without serum) by centrifugation (1500 rpm for 10 min). The cell pellets were resuspended in 0.2 cm^{-3} complete medium containing 1 μci/mL ^{3}H-thymidine and pulse labeled for 4 h. The cells were then washed thrice with phosphate buffer saline (PBS), lysed with 1% sodium dodecyl sulfate saline (SDS) and the lysate was counted for radioactivity in LKB-β/-liquid scintillation counter. The percentage inhibition of incorporation was calculated as follows:

$$\%\ \text{inhibition} = 1 - \frac{\text{CPM in treated tumor cells}}{\text{CPM in untreated tumor cells}} \times 100$$

Compounds

Preparation of [Na(*o*-HOdtb)] and [Bu^n_4N][*o*-HOdtb]: Sodium *o*-hydroxydithiobenzoate was prepared as reported elsewhere.[47] The solution of sodium orthohydroxy dithiobezoate in EtOH–H_2O (50% v/v) was made slightly acidic (pH 6–6.5) by the additon of AcOH diluted with H_2O. To this solution, an excess of the aqueous-ethanolic solution of *n*-tetrabutylammonium bromide (ca. 0.5 M) was added with stirring until precipitation occurred. The product was filtered off, washed with H_2O, dried and the crude Bu^n_4N(*o*-HOdtb) was recrystallized from warm EtOH and dried in vaccuo.

Preparation of H_2C(*o*-HOdtb)$_2$. When [Bu^n_4N][Zn(*o*-HOdtb)$_3$] was recrystallized from CH_2Cl_2 at room temperature, gave yellow crystalline solid with elemental analysis corresponding to H_2C(*o*-HOdtb)$_2$. The ^1H NMR spectrum shows a singlet at δ 5.1 ppm for methylene protons, multiplet in the region δ 6.8–7.9 ppm for aromatic protons and a broad signal at δ 10.6 ppm for phenolic proton. The crystallized product obtained, melted at 92 °C.

Preparation of the complexes: M(*o*-HOdtb)$_n$. A solution of Na(*o*-HOdtb) (ca. 1.92 g, 100 mmol) in ethanol (50 mL) was made slightly acidic (pH 6–6.5) by the addition of few drops of AcOH diluted with H_2O, was added to an aqueous-ethanolic/methanolic solution (50 mL, 50% v/v) of the appropriate metal(II) acetate or $FeCl_3$ in 2:1 molar ratio. Zn(II) and V(V) complexes could not be prepared from the sodium salt of o-hydroxydithiobenzoate, therefore, they were prepared from *n*-tetrabutylammonium salt of *o*-hydroxydithiobenzoate by the following method.

$ZnSO_4 \cdot 7H_2O$ (0.24 g, 1.48 mmol) and $VOSO_4 \cdot 2H_2O$ (0.45 g, 2.76 mmol) were dissolved in MeOH (~30 mL) and to it was added [Bu^n_4N][*o*-HOdtb] (in 40 mL warm MeOH) in 1:2 and 1:4 molar ratio, respectively, acidified with few drops of AcOH (pH 6–6.5). The reaction mixture was stirred at room temperature for ~30 min. The solvent was evaporated and the crude solids obtained were recrystallized from acetone.

Registry. The crystal structure data have been deposited to the Cambridge Crystallograpic Deposit Centre. Registry No. [Bu^n_4N][Zn(*o*-HOdtb)$_3$] CCDC 150588 and H_2C(*o*-Hodtb)$_2$ CCDC 150587.

References and Notes

1. Gale, E. F.; Cundlife, E.; Reynolds, P. E.; Richmond, M. H.; Waring, M. J. *Molecular Basis of Antibiotic Action*; John Wiley: New York, 1977; p 258.
2. Gniazdowski, M.; Cera, C. *Chem. Rev*. **1996**, *96*, 619.
3. Matsukage, A.; Hirose, F.; Yamaguchi, M. *Jpn. J. Cancer Res*. **1994**, *85*, 1.
4. Darzykieweiz, Z. Z. *Leukemia* **1998**, *2*, 777.
5. Marx, K. A.; Seery, C.; Malloy, P. *Mol. Cell. Biochem*. **1989**, *90*, 37.
6. Furst, A. *Chemistry of Chelation in Cancer*; Springfield, IL, 1963.
7. Schubert, J. *Sci. Am*. **1966**, *214*, 40.
8. Livingstone, S. E.; Mikhelson, A. E. *Inorg. Chem*. **1970**, *9*, 2545.
9. Ali, M. A.; Livingstone, S. E. *Coord. Chem. Rev*. **1974**, *13*, 101.
10. Das, M.; Livingstone, S. E. *Inorg. Chim. Acta* **1976**, *19*, 5.
11. Livingstone, S. E. *Coord. Chem*. **1980**, *20*, 141.
12. Das, M.; Livingstone, S. E. *Brit. J. Cancer* **1978**, *37*, 466.
13. Kaim, W.; Schwederski, B. *Bioinorganic Chemistry: Inorganic Elements in the Chemistry of Life—An Introduction and Guide*; John Wiley & Sons: New York, 1994; p. 364.
14. Singh, N. K.; Singh, A.; Sodhi, A.; Shrivastava, A. *Transition Met. Chem*. **1997**, *22*, 570.
15. Ferguson, J. *J. Chem. Phys*. **1964**, *40*, 3406.
16. Lever, A.B.P *Inorganic Electronic Spectroscopy*, 2nd ed.; Elsevier: Amsterdam, 1984.
17. Nakamoto, K. *Infrared and Raman Spectra of Inorganic and Coordination Compounds*; Wiley: New York, 1977; p 227.
18. Maltese, M. *J. Chem. Soc., Dalton Trans*. **1972**, 2664.
19. Burke, J. M.; Fackler, J. P., Jr. *Inorg. Chem*. **1972**, *11*, 3000.
20. Smith, T. D.; Pilbrow, J. R. *Coord. Chem. Rev*. **1974**, *13*, 173.
21. Mohan, M.; Gupta, N. S.; Gupta, M. P.; Kumar, A.; Kumar, M.; Jha, N. K. *Inorg. Chim. Acta* **1988**, *152*, 25.
22. Ashworth, C. C.; Bailey, N. A.; Johnson, M.; McCleverty, J. A.; Morrison, N.; Tabbiner, B. *J. Chem. Soc., Chem. Commun*. **1976**, 743.
23. Steinkopf, S.; Garoufis, A.; Nerdal, W.; Sletten, E. *Acta Chem. Scand*. **1995**, *49*, 495.
24. Watt, R. K.; Ludden, P. W. *Cell Mol. Life Sci*. **1999**, *56*, 604.
25. Krynetskaya, N. F.; Kubareva, E. A.; Timchenko, M. A.; Belkov, V. M.; Shabarova, Z. A. *Biochemistry (Mosc.)* **1998**, *63*, 1068.
26. Buttke, T. M.; Sandstrom, P. A. *Immunol. Today* **1994**, *15*, 7.
27. Ranjan, P.; Sodhi, A.; Singh, S. M. *Anticancer Drugs* **1998**, *9*, 333.
28. Rosenberg, B. *Cancer* **1985**, *55*, 2303.
29. Singh, S. M.; Parajuli, P.; Srivastava, A.; Sodhi, A. *Int. J. Immunopathol. Pharmacol*. **1997**, *1*, 27.
30. Deckers, P. J.; Davis, R. C.; Parker, G. A.; Mannick, J. A. *Cancer Res*. **1973**, *33*, 33.
31. Loeffler, C. M.; Smyth, M. J.; Longo, D. L.; Kopp, W. C.; Harvey, L. K.; Tribble, H. R.; Tase, J. E.; Urba, W. J.; Leonard, A. S.; Young, H. A.; Ochoa, C. *J. Immunol*. **1973**, *149*, 949.
32. Salitzeanu, D. *Adv. Cancer Res*. **1990**, *60*, 246.
33. Handy, C. C.; Balducci, L. *Am. J. Med. Sci*. **1985**, *290*, 196.
34. Kumar, A.; Singh, S. M. *Immunol. Cell Biol*. **1995**, *73*, 220.
35. Saryan, L. A.; Ankel, E.; Krishnamurti, C.; Petering, D. H. *J. Med. Chem*. **1979**, *22*, 1218.
36. Jeffery, G.H.; Bassett, J.; Mendham, J; Denney, R.C., *Vogel's Text Book of Quantitative Inorganic Analysis*, 5th ed.; ELBS, Longman: Singapore, 1989.
37. Programmes for diffractometer operation, data collection, data reduction and absorption correction were those supplied by Bruker.
38. Sheldrick, G. M. *Acta Crystallogr*. **1990**, *A46*, 467.
39. Sheldrick, G. M., *SHELXL-93. Programme for Crystal structure Refinement*; University of Gottingen: Germany, 1993.
40. Flack, H. D. *Acta Crystallogr*. **1987**, *A39*, 876.
41. Shanker, A.; Singh, S. M. *Tumor Biol*. **2000**, 591.

42. Parajuli, P.; Singh, S. M.; Kumar, A. *Int. J. Immunopharm.* **1995**, *17*, 1.
43. Mosamann, T. R.; Cherwinski, H.; Bond, M. V.; Giedliv, M. A.; Coffmann, R. *J. Immunol.* **1986**, *13*, 2348.
44. Shanker, A.; Singh, S. M. *Neoplasma* **2000**, *47*, 2.
45. Sellins, K. S.; Cohen, J. J. *J. Immunol.* **1987**, *139*, 3199.
46. Singh, N. K.; Srivastava, A.; Ranjan, P.; Sodhi, A. *Transition Met. Chem.* **2000**, *25*, 133.
47. Jenson, K. A.; Pederson, C. *Acta Chim. Scand.* **1961**, *15*, 1097.